JOURNAL OF GUIDANCE, CONTROL, AND DYNAMICS
Vol. 26, No. 5, September–October 2003

Probability of Midair Collision During Ultra Closely Spaced Parallel Approaches

Sharon W. Houck*
Seagull Technology, Inc., Campbell, California 95008
and
J. David Powell†
Stanford University, Stanford, California 94305

This research considers the technological components required in an aircraft to safely perform simultaneous, instrument approaches into an airport with parallel runways spaced less than 2500 ft apart. Monte Carlo simulations were used in order to assess the probability of collision during an unexpected aircraft blunder, but many of the input parameters such as flight technical error, navigation sensor error, and pilot time delay were based on recently generated experimental data. This analysis shows that with the Federal Aviation Administration's global positioning system-based Local Area Augmentation System operational and a reliable data link transmitting full state information between aircraft, it is technically feasible to reduce runway spacing to 1500 ft or less using the same safety criteria as that used for the recently implemented Precision Runway Monitor program.

Introduction

IN visual conditions simultaneous, parallel approaches can be made to runways that are a mere 700 ft apart, centerline to centerline, with air traffic control passing separation responsibilities to the pilots. This distance is just over three times the 212-ft wing span of a B-747-400. During instrument conditions, the minimum runway spacing for the same procedure is 3400 ft for airports with a Precision Runway Monitor (PRM) radar and 4300 ft for airports without a PRM radar. Air traffic controllers bear the responsibility to ensure adequate aircraft separation during instrument conditions and do so by reference to aircraft position derived from radar returns. Onboard aircraft position, frequently obtained by using the global positioning system (GPS), which is accurate to within 10 m (95%), is not transmitted to air traffic controllers nor to other aircraft. There is also no equipment in place by which to measure the location of aircraft wake vortices. On a visual, simultaneous parallel approach, wake vortex concerns are obviated by having the aircraft fly exactly or very nearly side by side.

Consider the information a pilot obtains visually about an adjacent aircraft. The pilot notes relative position and velocity and the attitude of the aircraft, and is rather certain that the intent is to follow the (visual) glideslope to a safe landing. If equivalent information about the approach and adjacent aircraft could be passed to the pilot or autopilot during instrument conditions, it would follow that the aircraft could continue to perform parallel approaches to the same safety level as that in visual conditions without visual contact. Even during visual conditions, a pilot cannot see the wake of the adjacent aircraft.

Technology and procedures that would permit the distance between parallel runways during an instrument approach to drop to that allowed during visual approaches would double the bad-weather capacity of an airport currently constrained to only single runway use during instrument conditions. With this goal in mind, this research set out to quantify the effect of improved technology on required runway spacing: specifically, the effects of improvements in navigation enabled by differential GPS, improvements in guidance through the use of advanced pilot displays and autopilots, and the introduction of new information to pilots on neighboring traffic made possible by air-to-air data links. Of particular importance to this research was the effort to obtain or create high-quality, experimental data on which to base a detailed Monte Carlo simulation.

This problem of allowing two airplanes to fly in close proximity to one another in the clouds while maintaining necessary safety margins has been addressed by numerous researchers over the past 10 years. Outstanding work has been accomplished by the Federal Aviation Administration (FAA)[1] and Massachusetts Institute of Technology (MIT)'s Lincoln Laboratories[2,3] on the Precision Runway Monitor Program, which successfully brought required runway spacing down to 3400 ft, and NASA Langley Research Center[4] and Honeywell[5] on the Airborne Information for Lateral Spacing program, which demonstrated techniques by which the required spacing can be further reduced to 2500 ft. Additional work has been performed by MIT,[6] the Cargo Airline Association,[7] Stanford University,[8] and Georgia Tech[9] to identify various techniques to increase airport capacity during instrument conditions, particularly taking advantage of the information proposed in the Airborne Dependent Surveillance-Broadcast (ADS-B) data link.

Rather than using historical databases for flight data, this research has created a new database of information on the accuracy to which pilots can fly their aircraft during instrument approaches. Also experimentally flight tested was pilot reaction time during formation flying maneuvers in order to simulate how quickly a pilot can react to an unexpected blunder from an adjacent aircraft. Data from Stanford and FAA flights on the demonstrated accuracy of differential GPS while airborne has also been compiled and used in this research. Not enough data were gathered to construct statistically significant results; however, the goal was to use demonstrated, realistic values for these parameters. There is no "padding" built into this analysis; instead Gaussian distributions are used where appropriate to allow both nominal and six-sigma cases. It can be argued that safety margins must be added in; if so, then they should be explicitly stated as that rather than inflating known values or distributions. The experimentally determined data on flight technical error, navigation sensor error, and pilot delay time were combined with models of aircraft roll dynamics, distributions of additional delay components, and distributions of realistic relative speed and longitudinal spacing differences. These probabilistic parameters were then incorporated into a two-airplane, ultra closely spaced parallel instrument

Received 8 March 2002; revision received 22 January 2003; accepted for publication 12 May 2003.

*Manager, Vehicle Sensors and Systems, 1700 Dell Avenue. Member AIAA.
†Professor Emeritus, Department of Aeronautics and Astronautics. Fellow AIAA.

approach Monte Carlo simulation with a fixed adjacent aircraft blunder trajectory commencing at 5 n miles from the runway threshold. These simulations included navigation capabilities with both the current instrument landing system and future differential GPS navigation systems in order to compare the different technologies and their effect on blunder avoidance. At least 100,000 trajectories were run for each scenario, with the miss distance (based on a B-747 fuselage length of 232 ft) recorded for each trajectory. This miss distance parameter is termed the closest point of approach. The resulting distribution of closest points of approach for the trajectories were then studied and the probability of collision during a blunder calculated for various approach guidance system/pilot interface combinations.

These resulting probabilities of collision during a blunder were then combined with the FAA's method of assessing the probability of a blunder occurring during any given approach to determine the overall likelihood of a collision for any given ultra closely spaced parallel approach. This probability was then compared with the FAA's acceptable values and conclusions made on the safety of parallel approaches to runways with spacings of 750, 1100, and 1500 ft.

Flight Technical Error Models

One of the key parameters to specify when modeling instrument approach procedures is the total system error, which is comprised of the navigation sensor error and the flight technical error. The navigation sensor error is a function of the instrument approach navigation system itself and the onboard installed equipment guiding the pilot or autopilot. The flight technical error is determined by how well the pilot or autopilot can follow the flight path indicated on the instruments. Not only is the flight technical error a function of the pilot's display in the case of a manual approach, but it is also a function of winds and turbulence.

Very little published experimental evidence exists that reports flight technical error or navigation error. Prior to differential GPS, "truth" was typically a laser-based system installed on the airport. With upcoming, aviation-certified, differential GPS systems such as the Wide Area Augmentation System (WAAS) and the Local Area Augmentation System (LAAS), the measured horizontal accuracy of the guidance system is on the order of 1–8 m, 95% of the time.[10] In fact, local-area differential GPS systems are now used as truth for certifying instrument landing systems. If using WAAS or LAAS as a guidance sensor, flight technical error, typically on the order of tens to hundreds of meters, would outweigh navigation sensor error by an order of magnitude. On-aircraft GPS systems are now accurate enough to digitally record flight technical error to within 5 m.

Because of the lack of available, accurate, experimental flight technical error data, differential GPS techniques were used to experimentally measure flight technical error during instrument approaches of a twin-engine, general aviation aircraft.[11] The primary variables investigated during these flights were approach path geometry and pilot display. Two types of approach paths were specified: 1) angular, such as that used by today's instrument landing system and 2) constant width, linear corridors such as might someday be specified by a differential GPS system. Two displays were presented to the pilot: 1) the standard course deviation indicator (commonly referred to as "the needles") and 2) a tunnel-in-the-sky display prototype. In addition to this pilot-in-the-loop data, position data from a B-757 autopilot during 15 simulated instrument approaches into NASA's Wallops Field were obtained and used as a basis for determining flight technical error for a state-of-the-art autopilot.

Time histories for two sets of approaches are presented in Figs. 1 and 2. Figure 1 presents data for nine angular, instrument landing system-like approaches using a course deviation indicator for the pilot's display. With the bias removed and using WAAS to determine position, the measured one-sigma standard deviation away from the approach centerline was 60 ft at 5 n miles. Figure 2 presents the results of four angular approaches, but uses the tunnel-in-the-sky display rather than the needles. The tunnel-in-the-sky display used WAAS to input the angular waypoints along the flight path and a prototype attitude heading system for roll, pitch, and yaw. The

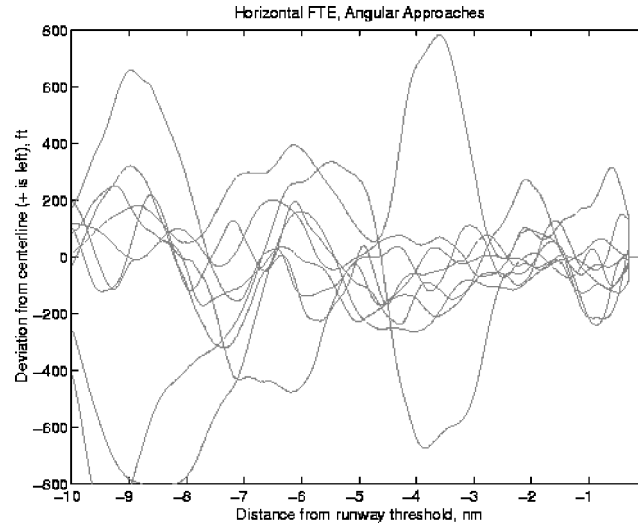

Fig. 1 Flight technical error vs distance from the runway for pilots using the course deviation indicator (needles) display.

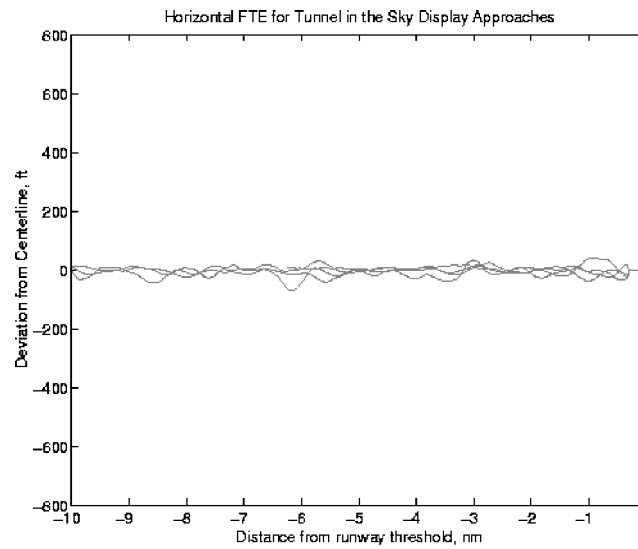

Fig. 2 Flight technical error with a tunnel-in-the-sky display.

WAAS measured deviation from approach centerline after the bias is removed has a one-sigma standard deviation of 16 ft, a marked improvement over the course deviation indicator. On each plot, flight technical error in feet is on the y axis vs distance from the airport in nautical miles. A positive flight technical error represents error to the left of centerline, whereas a negative flight technical error represents error to the right of the approach centerline. The scales on each plot are identical. The four-fold improvement in flight technical error is primarily caused by the improved piloting achievable with the tunnel-in-the-sky display compared to the needles. Flight tests were later carried out with the tunnel-in-the-sky display during light to moderate turbulence levels. Further details and results on these flights can be found in Houck et al.[11]

During instrument approaches, airline pilots frequently engage the autopilot. Therefore, not only is pilot-in-the-loop flight technical error important, but also that obtained with the autopilot engaged is important. Horzontal flight technical error from a Boeing 757 with the autopilot engaged during 15 instrumented approaches using a SCAT-1, local-area differential GPS navigation system is presented in Fig. 3. The bias has been removed, resulting in deviation from mean flight path on the y axis vs time since the start of the approach on the x axis. These data were obtained during the NASA Langley and Honeywell Airborne Information for Lateral Spacing flight tests.[5] The flights occurred in visual conditions with the test

Table 1 ICAO ILS permitted guidance errors

Approach position	ILS element	Category I Bias, ft (max)	Category I Bends, ft (95%)	Category I Total NSE, ft	Category II Bias, ft (max)	Category II Bends, ft (95%)	Category II Total NSE, ft	Category III Bias, ft (max)	Category III Bends, ft (95%)	Category III Total NSE, ft
Outer marker (5 n miles)	Glideslope	122	77	199	121	77	198	65	77	142
	Localizer	136	249	385	93	249	342	41	249	290
Inner marker (1000 ft)	Glideslope	8	5	13	8	3	11	4	3	7
	Localizer	42	37	79	29	12	41	13	12	25

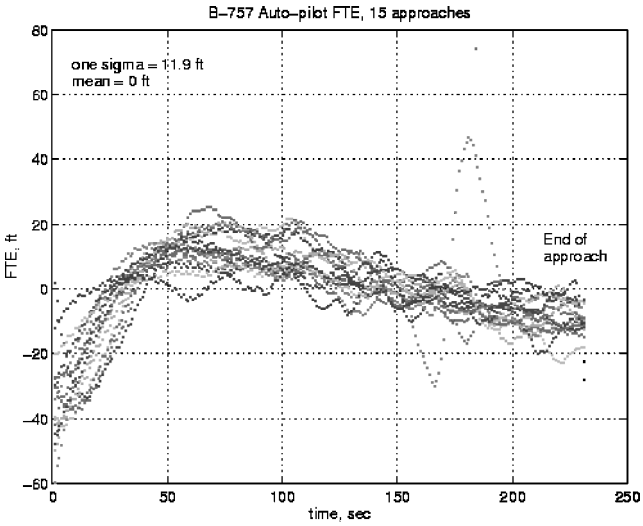

Fig. 3 Flight technical error for a B-757 with autopilot coupled during differential GPS-guided approaches.

pilot's view of the outside obstructed in order to simulate instrument conditions. For the 15 approaches the standard deviation is 11.9 ft, demonstrating extremely tight following of the flight path. No modifications were made to the production autopilot in these tests. Note that the single horizontal flight technical error excursion to 45 ft is unexplained. In the past analysts modeling instrument approach procedures have used at least 700 ft for flight technical error[12] alone, which is more than an order of magnitude higher than that demonstrated in these tests.

One of the major dilemmas in modeling flight technical error is how to account for atmospheric disturbances such as wind and turbulence. It is reasoned that although very low flight technical error numbers are now valid, a safety buffer must be incorporated into any analysis in order to account for atmospheric turbulence. This is valid, although increasing flight technical error from the demonstrated 32 ft to the currently used 700 ft (two sigma) can be excessively conservative. The Monte Carlo simulations in this research assumed a calm or steady wind day, with the implication that ultra closely spaced parallel approaches should not be performed in gusty, turbulent conditions. In the future turbulence simulations[13] using turbulence models from NASA Dryden Flight Research Center or MIL-STD 1797A can be incorporated into the present analysis in order to determine the maximum turbulence levels allowable to safely conduct these types of approaches.

Navigation Sensor Error Models

Navigation sensor error (NSE) is defined as the guidance error caused by the navigation system alone, including both ground-based and airborne components. Simply, the navigation system attempts to define a perfect path in the sky for a pilot to follow; however, every system has some inaccuracy. Navigation sensor error attempts to define the difference between the actual pathway in the sky and the desired, true pathway. Note that defining "truth" has always been a challenge.

Table 2 Coefficients for the LAAS airborne receiver noise model

Airborne model	a_0, m	a_1, m	θ_c, deg
AADA (worst)	0.15	0.43	6.9
AADB (best)	0.11	0.13	4.0

Instrument Landing System Navigation Sensor Error Model

The navigation sensors used in this study were the Category II Instrument Landing System (ILS) and Local Area Augmentation System (LAAS), the current and future U.S. precision approach guidance systems.

The ILS accuracy is driven by its sensitivity to the local environment. Multipath because of hangars, taxiing aircraft, and terrain cause bending or scalloping of the indicated glidepath. Additional interference caused by other radio-frequency sources reduces the accuracy of the ILS. The FAA's *Standard Flight Inspection Manual* defines the procedures for testing the accuracy of the ILS.[14] International Civil Aviation Organization (ICAO) standards for ILS accuracy are presented in Table 1.[15]

LAAS Navigation Sensor Error Model

The LAAS model used for this study is based on the Ground Accuracy Designator B (GADB) and Airborne Accuracy Designator A (AADA) models of LAAS, defined in McGraw et al.[16] and developed by researchers at several institutions. The accuracy, integrity, continuity, and availability of the GADB/AADA model are likely to be slightly worse than the final category I precision landing system supported by LAAS, and so it represents a worst-case LAAS NSE. The final NSE numbers were compared to a best-case category III model, GADC/AADB, to determine how inflated the final values might be. A summary of the LAAS NSE model follows. For each case a satellite elevation of 15 deg was used, and only one ground reference receiver calculated the differential correction. Combining these assumptions gives a reasonable, but conservative value of LAAS NSE.

The airborne receiver's pseudorange error is modeled as the rss of the thermal noise (n) and airframe multipath errors (mp),

$$\sigma_{\text{air}} = \sqrt{\sigma_n^2 + \sigma_{\text{mp}}^2} \tag{1}$$

where, for

$$\theta = 15 \text{ deg} \tag{2}$$

$$\sigma_n(\theta) = a_0 + a_1 e^{-\theta/\theta_c} \tag{3}$$

$$\sigma_{\text{mp}}(\theta) = 0.13 + 0.53e^{-\theta/(10 \text{ deg})} \tag{4}$$

The coefficients for Eq. (3) are given in Table 2 for the different airborne models. The ground reference receiver pseudorange error is modeled by

$$\sigma_{\text{gr}}(\theta) = \begin{cases} a_0 + a_1 e^{-\theta/\theta_c}, & \theta \geq 35 \text{ deg} \\ \sigma_{\max}, & \theta < 35 \text{ deg} \end{cases} \tag{5}$$

where the coefficients are presented in Table 3.

The troposphere and ionospheric pseudorange error models were included in the LAAS NSE model and will be broadcast as part of

Table 3 Coefficients for the overall LAAS ground-receiver pseudorange error model

Ground-station model	a_0, m	a_1, m	θ_c, deg	σ_{max}
GADA (worst)	0.50	1.65	14.3	——
GADC (best)	0.15	0.84	15.5	0.24

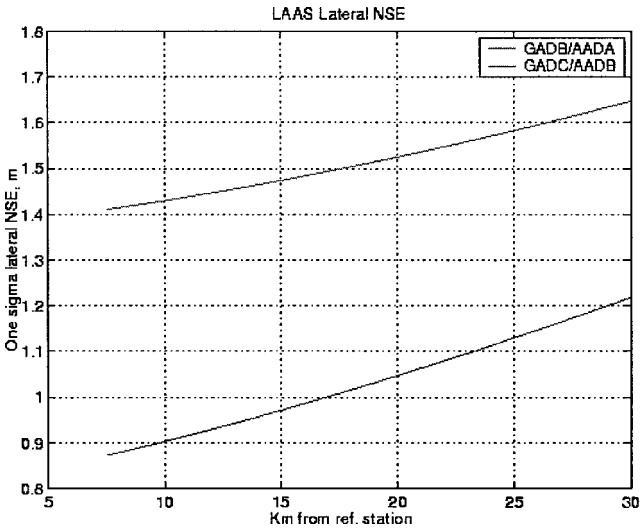

Fig. 4 LAAS navigation sensor error for two models.

the LAAS data-link message. The four components of the overall pseudorange error, airborne receiver thermal noise and multipath, ground receiver thermal noise and multipath, troposphere, and ionosphere errors, are root sum squared to obtain the final, modeled pseudorange error:

$$\sigma_{\text{pr}}(\theta, x_{\text{air}}, \Delta h) = \sqrt{\sigma^2_{\text{air}} + \sigma^2_{\text{grnd}} + \sigma^2_{\text{tropo}} + \sigma^2_{\text{iono}}} \tag{6}$$

To convert the pseudorange error into the position domain, the following equations are used:

$$\sigma_{\text{NSE}}(x_{\text{air}}) = \sigma_{\text{pr}}(x_{\text{air}}) \cdot \text{LDOP}$$

$$\text{LDOP} = 0.818 \cdot \text{VDOP}, \qquad \text{VDOP} = \frac{\text{VAL}}{5.8 \cdot \sigma_{\text{pr}}(7.5\ \text{km})} \tag{7}$$

where VDOP is the vertical dilution of precision, VAL is the vertical alarm limit maximum of 10 m, and the denominator in the VDOP equation is the smallest error in the range domain that poses an integrity threat when converted to vertical position. The 0.818 factor in the lateral dilution of precision (LDOP) equation comes from Nam et al.[17] and is a representative ratio between the standard deviations of the vertical and horizontal NSE components. The 7.5 km is a result of the approximate distance from the ground station to the runway threshold. This 7.5 km is then also added to the distance between the airplane and the runway threshold for purposes of computing lateral NSE. Figure 4 presents the lateral LAAS NSE for both models. The more conservative GADB/AADA model was used for the Monte Carlo simulations.

Navigation Sensor Error Summary

The Category II ILS flight technical error (FTE) assumes the bias in the ILS installation has been calibrated to near zero or to the outside of the dual-aircraft approach path. In the case of parallel runways, each with an ILS for guidance, each runway will produce a different NSE as each ILS installation is an independent guidance system. In the case of a single LAAS system serving multiple runways, the NSE will be approximately the same for each runway because the same GPS satellites will be used to create the differential corrections. It is assumed that both airplanes will be observing the same GPS satellites while on simultaneous approaches.

Table 4 NSE and FTE for Monte Carlo study

Parameter	1 σ value, ft
Piloted FTE	16
Autopilot FTE	11.9
ILS NSE	132
LAAS NSE	4.9

Table 5 B-747 data

Parameter	Value
I_x, slug $\cdot$ ft^2	18.2e6
Wing area S, ft^2	5500
Wing span b, ft	195.68
C_{l_p}	−0.45
$C_{l_{\delta a}}$	0.0461

The Monte Carlo simulations that follow use the experimentally obtained flight technical error results from the piloted, tunnel-in-the-sky approaches in the twin-engine, general aviation aircraft (a Beechcraft Queen Air) and the autopilot data from the B-757. The ILS and LAAS navigation sensor errors were modeled as Gaussian distributions with the modeled category II ILS lateral NSE one-sigma error being 132 ft and the LAAS one sigma being 4.9 ft. These numbers are based on NSE allowed for a category II ILS just outside 5 n miles from the runway threshold and a category I type of LAAS model at 5 n miles. The navigation sensor error and flight technical error data are summarized in Table 4.

Aircraft Model

Rather than modeling the aircraft roll response for the blunder and evasion maneuvers as an instantaneous roll rate, the roll-rate time history for a given aileron input for both the evader and blunderer airplanes was calculated using linearized aerodynamic coefficients for an older model B-747. Table 5 presents the geometric and aerodynamic data for the B-747 from Etkin and Reid.[18]

Beginning with the linearized, small-perturbation aircraft dynamic equations of motion, assuming x–z plane symmetry and simple roll without perturbation in the other axes,

$$\frac{\partial L}{\partial \delta_a}\Delta\delta_a + \frac{\partial L}{\partial p}\Delta_p = I_x \Delta\dot{p} \tag{8}$$

where L is rolling moment, δ_a is aileron deflection, p is roll rate, I_x is moment of inertia in the x plane, $\dot{p}$ is roll acceleration, and $(\partial L/\partial\delta_a)\Delta\delta_a$ is the roll moment caused by the deflection of the ailerons and $(\partial L/\partial p)\Delta p$ is the roll-damping moment. Equation (8) can be rewritten as

$$\tau\Delta\dot{p} + \Delta p = -L_{\delta a}\Delta\delta_a / L_p \tag{9}$$

where

$$\tau = -\frac{1}{L_p}, \qquad L_p = \frac{QSb^2C_{l_p}}{2I_x u_0}, \qquad L_{\delta a} = \frac{QSbC_{l_{\delta a}}}{I_x} \tag{10}$$

and τ is defined as the roll mode time constant, Q is the dynamic pressure, and u_0 is the airspeed. For a step change in aileron deflection, Eq. (9) can be analytically solved to produce

$$\Delta p(t) = -(L_{\delta a}/L_p)(1 - e^{-t/\tau})\Delta\delta_a \tag{11}$$

To generate the desired maximum 10 deg/s roll rate, a step composite aileron input of 40 deg was specified, and the roll-rate time history proceeded from Eq. (11) and is shown in Fig. 5. The roll responses of both the evading and blundering aircraft were modeled in this way.

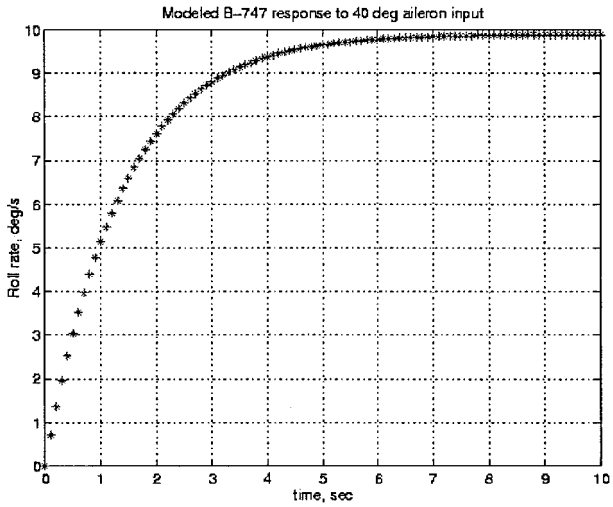

Fig. 5 Time history of roll angle of modeled B-747 with 40-deg aileron input.

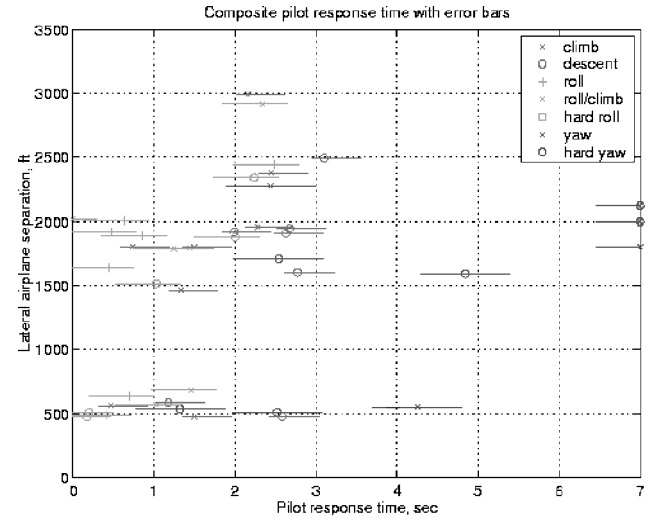

Fig. 6 Composite of pilot response times with error estimations.

Delay Models

Prompt response to a blunder is critical to avoiding a collision and is probably the key difference between visual and instrument flying. Rather than seeing the adjacent aircraft, the pilot or autopilot must be presented with sufficient information quickly in order to diagnose and respond to an unseen blunder. This results in generally longer response times. The overall delay time can be broken up into the following components: 1) pilot or autopilot response time, 2) data-link update rate and collision detection and resolution time, 3) antenna/computer electronics delay, and 4) electromechanical actuator delay. Each were determined to be either a fixed delay time or were assigned a uniform distribution based on experimental data or analysis.

Human Pilot Delay

As with flight technical error, very little actual experimental data on pilot response time to an adjacent aircraft's movement exists. How the pilot determines that the adjacent aircraft has moved, how far, and in what direction is its anticipated trajectory are also unknown. An experimental evaluation of pilot-in-the-loop, dual-aircraft cruise formation flying system dynamics in visual conditions was undertaken to examine pilot response time as a function of lead aircraft maneuver and initial separation.[19] Various maneuvers such as rolls, climbs, descents, and wings-level yaws were performed by the lead aircraft. The trail pilot's task was to attempt to maintain the current separation distance by following the lead's maneuver. These maneuvers were then repeated at a closer range in order to model the pilot's response also as a function of initial separation distance. Results of these tests are presented in the composite graph of pilot response time to roll, pitch, and yaw maneuvers presented in Fig. 6. Error bars around each test point delineate the possible range of pilot response. See Houck and Powell[19] for further details on the test results.

One can see that the pilot generally responds the fastest to bank angle changes, followed by pitch changes, and is least responsive to heading angle changes. Both pitch and heading angle changes exhibit some sensitivity to separation distance; however, pilot response to bank angle change at separation distances less than 2000 ft is consistently less than 2 s. Beyond 2000 ft, pilot response is slower by half a second, but the quantity of data beyond 2000 ft is significantly less, and additional data should be obtained before direct comparison made.

The preceding experiments suggest that a pilot discerns bank angle change more quickly than either pitch or yaw angle change. The response time to a change in roll averages about 1 s for separations less than 2000 ft. Response to a climb maneuver is faster than that to a descent and is probably because pitching the nose up to climb is a more natural response than pushing over in order to descend. Pilot response to a wings-level yaw maneuver is between 1 and 5 s, but frequently there is no response at all. This series of flights forms a basis for analyzing pilot response; however, additional issues such as individual differences in pilot response, differences in lead aircraft maneuver entry characteristics, and atmospheric factors such as sun angle, background terrain, and cloud coverage have not been addressed.

Data from NASA Langley's AILS flight tests[5] demonstrated an average pilot response time of 0.3 s to a computer-generated collision alert during simulated instrument conditions at a 2500 ft separation distance, with a maximum response time of 1.0 s. Average reaction times demonstrated in the simulator studies of Abbott and Elliott[20] were 0.84 s for the same scenarios of the flight test, with a maximum of 1.84 and a minimum of 0.12 s, demonstrating that more than displays and aural warnings impact the human in the loop. Experimental results from Fig. 6 showed a maximum pilot delay time of 2 s for a roll maneuver. This includes the delay from yoke movement to control surface actuation.

Unpublished data on pilot response times being used in parallel approach certification today are on the order of 5 to 10 s. Some of this delay can be attributed to time required to reconfigure the airplane prior to executing the missed approach. However, in our judgment a pilot on an ultra closely spaced parallel approach would begin the escape maneuver immediately and reconfigure once a safe distance from the intruding airplane, just as would occur today in visual conditions at an airport such as San Francisco during parallel approaches. Based on the Stanford flight and NASA Langley simulator data, a uniform distribution ranging from 0.3 to 2.0 s was used to model the pilot response time to a blundering aircraft.

Autopilot Delay

For the Monte Carlo cases with the autopilot coupled, not only is the autopilot coupled during the approach but it remains in control of the aircraft throughout the emergency escape maneuver. This is termed an "intelligent" autopilot. During this time, the pilot monitors the aircraft systems as is currently done during an approach. For the intelligent autopilot approach and escape maneuver it is assumed that the autopilot has immediate access to the results of the collision detection algorithm and can react to an emergency escape maneuver in less than 100 ms. The autopilot must then either activate the yoke or electronically signal the actuators to begin the escape maneuver. Moving the yoke causes more delay than directly signalling the actuators, so that this case is modeled by a 0.5-s delay, for a fixed delay time of 0.5 s caused by the autopilot.

Delay Caused by Electronics and Actuators

The antenna/computer electronics delay and the electromechanical actuator delay were each assigned fixed quantities. These two

Table 6 Components comprising the total delay distributions

Parameter	Delay, s
Antenna/computers (fixed)	0.5
Electromechanical actuators (fixed)	0.5
Pilot reaction time (uniform distribution)	0.3–2.0
Autopilot reaction time (fixed)	0.5
Data-link/collision detection delay (uniform distribution)	1.0–2.0

quantities are based on known lags in computer processing times as well as actuator response times. Based on conversations held with personnel at the FAA Mike Munroney Aeronautical Center, the electronics delay was chosen to be 0.5 s. The electromechanical actuator delay time, defined as the delay from the initial movement of the yoke to the onset of positive roll rate, was also estimated to be 0.5 s.

Delay Caused by Data Link and Collision Detection

The data-link update rate directly affects the collision detection algorithm as it contains the necessary information to estimate aircraft trajectories. To prevent a high probability of false alarms, it is estimated that at least two updates from "anomalous" adjacent airplanes states will be required before onboard collision detection algorithms will determine that an escape maneuver is required. Using one Hz ADS-B as the baseline data link,[21] the minimum time to update the aircraft states twice is slightly over 1.0 s, assuming the start of the blunder occurs just before an update. Note that this means the blundering aircraft could not have moved very far nor changed its velocity vector to any significant degree, which implies that roll and roll rate might be required parameters in the data link in order to infer intent. However, as a minimum bound the data-link delay is estimated to be 1.0 s. At a maximum the onset of the blunderer's roll rate will occur immediately after the transmission of the aircraft states, causing a delay of 2.0 s as a result of the update rate. Although a higher update rate data link can be employed for ultra closely spaced parallel approaches, the blundering aircraft must still have time to exhibit a trajectory change sufficiently severe to be called a blunder, so 1 to 2 s for the range of possible delay caused by data link and collision detection is still considered reasonable if intent information such as roll angle and roll rate is also available.

Summary of Delay Times

A summary of the components of the total delay distribution is presented in Table 6. Either the autopilot or the pilot reaction time is used in each simulation; they are not used together.

Longitudinal Position Distribution

Videotaped observations of simultaneous, visual parallel approaches into San Francisco airport made by this author demonstrated that the longitudinal spacing can vary widely from approach to approach. Often, the approaches resembled dependent approaches (diagonal spacing 2 n miles or more) rather than simultaneous approaches. Although future autopilots might have the precision necessary to bring two aircraft to positions exactly abeam each other, it is likely that there will be some permitted longitudinal position variation that does not constitute a wake vortex hazard. For this study a uniform distribution of ± 500 ft was used to determine the initial longitudinal relative position of the blundering aircraft at the start of the blunder.

Airspeed Distribution

So as not to limit the study to exactly matched aircraft, the relative velocity of the evading aircraft was modeled as a uniform distribution with values between ± 20 kn from that of the blundering aircraft at the start of the blunder, allowing for differing approach speeds.

Summary of Monte Carlo Parameters

For each simulation run the following variables were randomly sampled from either a Gaussian or uniform distribution, as described in the preceding sections: 1) flight technical error for each aircraft (Gaussian), 2) navigation sensor error for each aircraft (Gaussian), 3) pilot reaction time (uniform), 4) data-link/collision detection delay time (uniform), 5) longitudinal relative position (uniform), and 6) relative airspeed (uniform).

The deterministic variables were set at the following values: 1) blunderer airspeed (140 kn), 2) maximum roll rate (10 deg/s each aircraft), 3) maximum roll angle (30 deg each aircraft), 4) maximum heading change (30 deg blunderer, 45 deg evader), 5) actuator and antenna delay time (1.0 s), and 6) autopilot reaction time (0.5 s).

Two-Dimensional, Ultra Closely Spaced Parallel Approach Model

Evader–Blunderer Model

The model created for the Monte Carlo analysis defines a continuous, two-dimensional, nonlinear, time-dependent trajectory for two point masses possessing kinematic airplane properties, with the exception of modeled aircraft roll response. One airplane is designated the blundering aircraft or "blunderer," and the second is designated as the evading aircraft or "evader." Two virtual runways are defined in an inertial reference frame while the aircraft trajectories are propagated in a leader/follower, translating, rotating, relative reference frame. The origin of the runway-referenced frame is placed at the approach end of the runway of the evader; the origin of the relative reference frame is the center of mass of the evader aircraft. After numerical integration of the equations of motion, a coordinate transform is performed at each time step to calculate both the relative and inertial positions and velocities of the airplanes.

The input vector contains initial conditions and maximum allowable values of the state vector. Additional conditions included are timing specifications and threshold values for maneuver initiation and termination. The model output is the complete time-dependent trajectory of the state vector, the closest point of approach of the two airplanes, and the time at which the closest point of approach occurred.

The evader airplane referenced coordinate frame is a lead/trail concept.[22] The origin of the relative frame is the translating and rotating center of mass of the evader airplane, shown in Fig. 7. The x direction is out the nose, and the positive y direction out the right wing of the evader aircraft. Ignoring the Earth's rotation and without loss of generality, the inertial frame (denoted by capital X and Y) is translating with the evader airplane. The local body-referenced frame (denoted by lowercase x and y) is used for intermediate calculations involving the relative rotation rates of the two airplanes.

Using this geometry, the differential equations of motion of the blunderer airplane relative to the inertial frame of the evader airplane are presented in Eqs. (12–14):

$$\dot{Y}_{\mathrm{B,Rel}} = V_B \sin(\Psi_B - \Psi_E) - \dot{\Psi}_E X \tag{12}$$

$$\dot{X}_{\mathrm{B,Rel}} = V_B \cos(\Psi_B - \Psi_E) - V_E + \dot{\Psi}_E Y \tag{13}$$

$$\dot{\Psi}_B(t) = \int \frac{g \tan\phi_B(t)}{V_B}\,\mathrm{d}t, \qquad \dot{\Psi}_E(t) = \int \frac{g \tan\phi_E(t)}{V_E}\,\mathrm{d}t \tag{14}$$

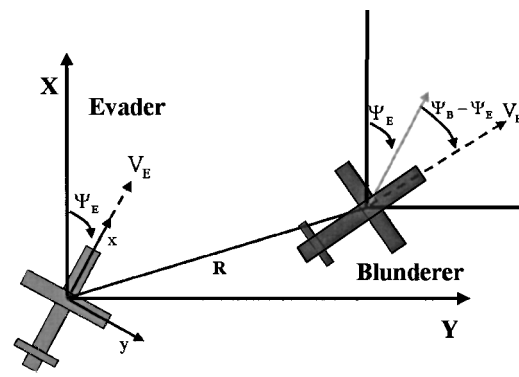

Fig. 7 Evader-reference relative frame.

Table 7 Probability of collision during a blunder (95% confidence interval ±0.3%)

Case	Piloted with tunnel-in-the-sky guidance FTE: $1\sigma = 16$ ft delay = 0.3 to 2.0 s	Intelligent autopilot with auto-escape FTE $1\sigma = 11.9$ ft delay = 0.5 s	LAAS $1\sigma = 4.9$ ft	ILS $1\sigma = 132$ ft	P(collision), % 750 ft	1100 ft	1500 ft
A	X	——	X	——	5.857	0	0
B	——	X	X	——	0.001	0	0
C	——	X	——	X	8.9940	0.17	0

where $\dot{X}_{B,Rel}$ and $\dot{Y}_{B,Rel}$ are the relative X and Y velocities of the blunderer with respect to the reference frame attached to the center of mass of the evader, $\dot{\Psi}_E$ is the heading rotation rate of the evader aircraft (positive clockwise), $\Psi_B - \Psi_E$ is the relative angle between the velocity vectors of the two aircraft, ϕ_E and ϕ_B are the roll angles of the evader and the blunderer (right roll being positive), g is the gravitational constant, and V_E and V_B are the airspeeds of the evader and blunderer, respectively. Note that $\dot{X}_{B,Rel}$ and $\dot{Y}_{B,Rel}$ are relative to the evader aircraft's center of mass and are independent of runway location.

To position the aircraft relative to a fixed set of runways, an inertial runway-referenced coordinate frame was used with a fixed origin at the threshold of the evader's intended runway. Once the runway-referenced position of the evader and the relative position of the blunderer to the evader are calculated, the position of the blunderer relative to its runway can be calculated by rotating and translating its position into the runway frame using Eqs. (15) and (16):

$$X_B(t) = X_E(t) + X_{B,Rel}(t)\cos -\Psi_E(t) + Y_{B,Rel}(t)\sin[-\Psi_E(t)] \quad (15)$$

$$Y_B(t) = Y_E(t) + \{-X_{B,Rel}(t)\sin[-\Psi_E(t)] + Y_{B,Rel}(t)\cos[-\Psi_E(t)]\} \quad (16)$$

The state vector is numerically integrated using a fourth-order Runge–Kutta method.

Baseline Blunder Scenario

Choosing a "nominal" blunder presents a challenge as there have been no reported blunders. Anecdotal evidence suggests that it is possible for an airplane to overshoot the runway centerline during lineup for the approach, to line up on the wrong runway, or to execute an improper missed approach by flying towards the adjacent airplane. In short, there is no a priori knowledge of the exact blunder. For the purposes of this analysis, the blundering aircraft's trajectory is based on the 30-deg blunder scenario used in NASA's Airborne Information for Lateral Spacing program. At 5 n miles from the runway, the blunderer rolls to a maximum rate of 10 deg/s to a maximum bank angle of 30 deg toward the evader with a maximum heading change of 30 deg. Note that this is an extreme blundering maneuver used for analytical cases and is not based on any documented, actual blunders. The evader then performs an escape maneuver consisting of rolling to a maximum rate of 10 deg/s to a maximum bank angle of 30 deg and a maximum heading change of 45 deg. This escape maneuver is similar to the climbing turn trajectory proposed by MIT,[6] but in two-dimensional form.

Monte Carlo Results

At each runway spacing of 750, 1100, and 1500 ft, 100,000 trajectories were run with the parameters described in the preceding sections. For each trajectory the closest point of approach was calculated, and if this distance was less than the B-747-400 fuselage length of 232 ft this was counted as a collision. At the end of the 100,000 runs, the total number of collisions was divided by the total number of runs, resulting in the probability of collision during a blunder for that runway spacing. Table 7 presents the results of the Monte Carlo runs for the various configurations and defines the three cases: A, B, and C. A plot of the probability of collision vs runway spacing for each case is presented in Fig. 8.

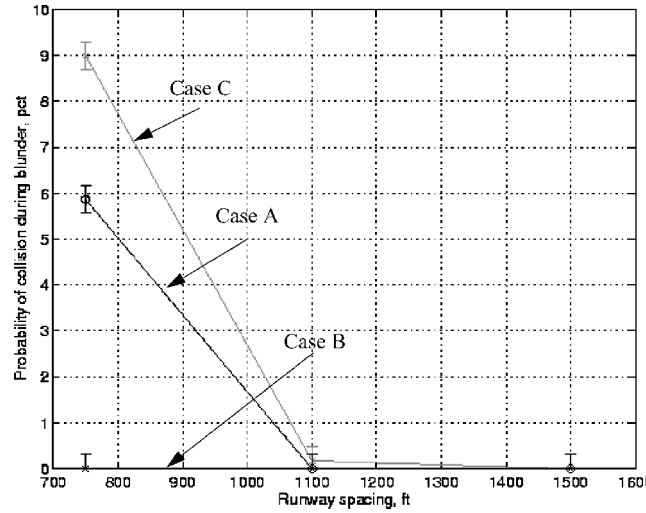

Fig. 8 Probability of collision during a 30-deg blunder for various sensor/pilot combinations.

It must be emphasized that additional onboard equipment is required for each case, as well as presumed enhancements to the existing GPS system, as discussed in preceding sections. In summary, the piloted cases assume 1) tunnel-in-the-sky guidance, which currently relies upon LAAS for position and velocity; 2) an attitude-heading reference system for attitude information; 3) an inertial measurement unit for smoothing position, velocity, and attitude; and 4) full state information on the adjacent aircraft along with collision detection ability. The autopiloted cases assume 1) computerized collision detection and resolution with the autopilot in control throughout all maneuvers and 2) full state information on the adjacent aircraft.

Because the probability of collision during a blunder calculation is a binomial random variable (it either collides or it does not), the Central Limit Theorem theorem can be used for large numbers of trials to make a Gaussian approximation to the 95% confidence interval around the calculated probability of collision. The binomial random variable is a sum of independent, identical Bernoulli random variables[23] with finite mean and variance, and in the limit the Bernoulli cumulative distribution function approaches that of the Gaussian. For the 100,000 total runs, in each case the 95% confidence interval that P(collision) is the true value is ±0.3103%.

Using today's ILS, the calculated probability of collision during a 30-deg blunder is 9% with 750 ft of runway separation, even assuming the best possible guidance system in the aircraft and advanced data links providing excellent information on the neighboring traffic. This is clearly unacceptable and illustrates one of the reasons why closely spaced approaches are not possible with the current system providing the navigation. Increasing the runway spacing to 1100 ft yielded 170 collisions out of 100,000 trials with blunders when using the ILS, which is still problematic. However, it appears from the study that 1100-ft spacing would be acceptable if navigation is provided by a system with the accuracy of LAAS. The airplanes can be manually flown with advanced displays, or the "intelligent autopilot" can be engaged; however, the airplanes are

Table 8 Estimated number of years between accidents during UCSPAs, given the *P*(collision) in Table 7[a]

Case	Piloted with tunnel-in-the-sky guidance FTE $1\sigma = 16$ ft delay = 0.3 to 2.0 s	Intelligent autopilot with autoescape FTE $1\sigma = 11.9$ ft delay = 0.5 s	LAAS $1\sigma = 4.9$ ft	ILS $1\sigma = 132$ ft	Number of years between accidents 750 ft	1100 ft	1500 ft
A	X	——	X	——	1.7	33	33
B	——	X	X	——	25	33	33
C	——	X	——	X	1.1	21.3	33

[a]Anything 25 years or greater meets the FAA safety criteria established during the PRM certification.

Table 9 Minimum component requirements for 750- and 1100-ft runway spacing

Navigation sensor	Human–machine interface	Traffic information required	Minimum runway spacing, ft
Cat I LAAS	Tunnel in the sky (requires LAAS, attitude, and inertial sensors), pilot reaction time 0.3 to 2 s	Full state information on adjacent traffic (position, velocity, attitude)	1100
Cat I LAAS	Intelligent autopilot in control throughout approach and escape maneuver	Full state information on adjacent traffic (position, velocity, attitude)	750

required to be equipped with an advanced data link that provides the position, velocity, roll angle, and roll rate of the neighboring traffic. To achieve a low probability of collision during a blunder (0.01%) at a runway spacing of 750 ft, it is necessary to use the intelligent autopilot to reduce reaction time, LAAS for low total system error, and the advanced data link, which provides complete information on the adjacent traffic.

Ultra Closely Spaced Parallel Approach Safety

Using the results of the Monte Carlo simulation and an estimate of the current safety level for instrument approaches, one can calculate the acceptable blunder frequency for ultra closely spaced parallel approaches. According to the FAA, if this blunder frequency is less than an intuitively reasonable number then ultra closely spaced parallel approaches (UCSPA) can be conducted with acceptable risk levels.

From data obtained between 1983 and 1988, there were two accidents during an estimated total of five million approaches. This reduces to an accident rate of one per 2.5 million approaches. During the PRM program,[1,24] the FAA identified nine potential causes of accidents during a final approach and added a blunder during a PRM approach as a tenth. Thus, if the current accident rate of one per 2.5 million approaches is to be maintained it was approximated that a blunder contributes one-tenth toward that accident rate. Therefore, the accident rate caused solely by blunders during a PRM can be no greater than one per 25 million approaches. At roughly one million approaches being performed per year, one accident every 25 years as a result of a blunder during an approach is acceptable. This is the specification that we will apply to UCSPA. It is difficult to estimate the number of unrecoverable blunders during any given year. "Unrecoverable" means that the airplane did not merely overshoot and correct back to centerline, but that the airplane blundered into the path of the adjacent airplane. Few, if any, of these unrecoverable blunders have ever been officially reported; however, based on anecdotal evidence, an estimate of 10 per year (in the United States) would be a conservative estimate.

A summary of the safety data calculated from the Monte Carlo data is presented in Table 8. The Monte Carlo data for 1500-ft runway spacing showed no collisions during blunders; however, the 95% error band is 0.3% or 0.003 collisions per blunder. Using this collision rate and based on the estimate of 10 unrecoverable blunders per year, this results in 0.03 collisions per year or one accident every 33 years. This is better than the safety criteria of one accident every 25 years.

At 1100-ft runway spacing with LAAS as the guidance system, the accident rate is also one every 33 years, also bettering the one every 25 years safety criteria. At 1100-ft runway spacing with ILS and an intelligent autopilot, the accident rate is one every 21.3 years, slightly worse that the one-per-25-years requirement.

At 750-ft runway separation LAAS with an intelligent autopilot combination results in one accident every 25 years, matching the acceptable safety criteria. At 750-ft runway separation with LAAS and a pilot in the loop, the result is one accident every 1.7 years. And with ILS and an intelligent autopilot the result is one accident every 1.1 years. Clearly, these last two configurations do not meet the accident rate criteria.

Although 10 blunders occurring per year is an admitted estimate, if the actual number were two times higher the accident rate would not change substantially. If the actual number of blunders were on the order of 100, there would be many more reported than what is evident today.

Discussion

This analysis demonstrates that ultra closely spaced parallel approaches are technically achievable using upcoming advanced navigation systems, data links, and pilot interfaces. The existing runway spacing requirement of 4300 or 3400 ft can be substantially reduced, to the levels of 1100 or 1500 ft, based on the FAA minimum safety requirements for a simultaneous, dual-aircraft instrument approach. The critical underlying technical presumptions of this research, differential GPS, air-to-air and air-to-ground data links, and a good autopilot or pilot interface, have all been successfully demonstrated in flight test by either this researcher or other researchers. Yet to be designed and tested is an intelligent autopilot that autonomously executes the emergency escape maneuver without pilot intervention. At least one collision detection algorithm has been successfully flight tested, and several are in work. Most of these algorithms assume aircraft attitude as well as three-dimensional position and velocity will be available in the data link. Given the tight requirements on minimizing the response time of the evading aircraft during a blunder, the collision detection community might well require a data-link update rate greater than 1 Hz in order to provide adequate collision diagnosis during an ultra closely spaced parallel approach while minimizing the false alarm rate. A summary of the components required to achieve 750- and 1100-ft runway separations for two nominal B-747 aircraft within the acceptable FAA safety margins is presented in Table 9.

The technology for ultra closely spaced parallel approaches will require new equipment in aircraft and on the ground. It will be such that both aircraft on a simultaneous approach will need to be equipped with the new technology, which means that most aircraft using an airport will need to be equipped in order to reap the full capacity benefits. The equipment and retraining will probably cost on the order of $200,000 per aircraft. The airframe manufacturers and their airline customers would save money if the airports footed the bill for wider runway spacing, thus not requiring aircraft reequipage and pilot training; however, a cost benefit study of the best overall solution for the taxpayers, the airline passengers, and freight shippers

who ultimately have to pay for the full system costs including airport expansions needs to be carried out to consider all alternatives. The study also should take into account the welfare of airport neighbors, residents of areas that might become new airports, and the environmental damage brought by expanding airports into areas that are now water. To put this into perspective, the reequipage of 10,000 aircraft (the current U.S. commercial fleet) would cost approximately two billion, whereas the expansion of San Francisco Airport into the Bay for new runways is projected to cost more than two billion! And this is just one proposed airport expansion project. In short, development of technology that allows the use of very closely spaced runways in instrument conditions might have significant long-term environmental and cost benefits.

Conclusions

This research combined Monte Carlo simulations with recently obtained high-quality flight test data to examine the technological components necessary for achieving simultaneous parallel approaches to runways spaced less than 2500 ft apart. Using the industry-accepted 30-deg turn blunder scenario and a safety criteria of one collision every 25 years used by the FAA for the Precision Radar Monitor program, this research demonstrates that ultra closely spaced parallel approaches are technically achievable at 1500 ft and in some cases 1100 ft in calm wind conditions. The main technological components necessary to achieve this is the Local Area Augmentation System, an air-to-air data link with full aircraft state information broadcasting reliably at 1 Hz, and either a three-dimensional perspective display for pilot-in-the-loop approaches or an intelligent autopilot that automatically executes an escape maneuver. All of the technologies except the intelligent autopilot have been demonstrated in the civilian aviation world. Ultra closely spaced parallel approaches would significantly reduce the need for airport runway expansion and its resulting adverse environmental impact. Though additional issues such as separation responsibility, wake-vortex avoidance procedures, and certification of new equipment are major drivers in the commercial aviation world, the technology is available either now or within the next five years to safely perform ultra closely spaced parallel approaches.

Acknowledgments

The financial support of this research from the FAA, Zonta International, and the American Association of University Women is greatly appreciated. The authors are indebted to Terry Abbott and Dawn Elliott of NASA Langley Research Center, James Kuchar of Massachusetts Institute of Technology, Amy Pritchett of Georgia Tech, and Claire Tomlin and Rodney Teo of Stanford for providing counsel, encouragement, and data, and consider this present work to have been built upon the excellent work that has preceded it.

References

[1]"Precision Runway Monitor Demonstration," DOT/FAA/RD-91/5, Cambridge, MA, Feb. 1991.

[2]Owen, M., "The Memphis Precision Runway Monitor Program Instrument Landing System Final Approach Study," Rept. DOT/FAA/NR-92/11, Cambridge, MA, May 1993.

[3]Shank, E., and Hollister, K., "Precision Runway Monitor," *Lincoln Laboratory Journal*, Vol. 7, No. 9, 1994.

[4]Elliott, D., and Perry, R., "NASA Research for Instrument Approaches to Closely Spaced Parallel Runways," AIAA Paper 2000-4358, Aug. 2000.

[5]Jackson, M., Samanant, P., and Haissig, C., "Design and Analysis of Airborne Alerting Algorithms for Closely Spaced Parallel Approaches," AIAA Paper 2000-4359, Aug. 2000.

[6]King, B., and Kuchar, J., "Evaluation of Collision Alerting Sytem Requirements for Paired Approach," *Proceedings of the 19th Digital Avionics System Conference*, Inst. of Electrical and Electronics Engineers, New York, 2000.

[7]Cargo Airline Association, FAA SafeFlight 21, "Phase I: Operational Evaluation," Final Rept., Washington, DC, April 2000.

[8]Teo, R., and Tomlin, C., "Computing Provably Safe Aircraft to Aircraft Spacing for Closely Spaced Parallel Approaches," *Proceedings of the 19th Digital Avionics System Conference*, Inst. of Electrical and Electronics Engineers, New York, 2000.

[9]Landry, S., and Pritchett, A., "The Safe Zone for Paired Closely Spaced Parallel Approaches: Implication for Procedures and Automation," *Proceedings of the 19th Digital Avionics System Conference*, Inst. of Electrical and Electronics Engineers, New York, 2000.

[10]"Minimum Operational Performance Standards for the Wide Area Augmentation System," RTCA/DO-229B, Washington, DC, 1999.

[11]Houck, S., Barrows, A., Parkinson, B., Enge, P., and Powell, J. D., "Flight Test of WAAS for Use in Closely Spaced Parallel Approaches," *Proceedings of the Institute of Navigation's GPS Conference*, 1999, URL: http://waas.stanford.edu/~wwu/papers/gps/pubs_chron.html [cited 6 Jan 2003].

[12]"Minimum Operational Performance Standards for Airborne Supplemental Navigation Equipment Using GPS," RTCA/DO-208, Washington, DC, July 1991.

[13]Yeager, J. C., "Implementation and Testing of Turbulence Models for the F18-HARV Simulation," NASA/CR-1998-206937, Edwards AFB, CA, March 1998.

[14]*US Standard Flight Inspection Manual*, Federal Aviation Administration, Order 8200.1A, Washington, DC, May 1996, revised July 2000.

[15]Kayton, M., and Fried, W., *Avionics Navigation Systems*, 2nd ed. Wiley Interscience, New York, 1997.

[16]McGraw, G., Murphy, T., Brenner, M., Pullen, S., and Van Dierendonck, A., "Development of the LAAS Accuracy Models," *Proceedings of the Institute of Navigation's GPS Conference*, Inst. of Navigation, Fairfax, VA, 2000.

[17]Nam, Y., Zalesak, T., Clark, B., Murphy, T., Anderson, L., and DeCleene, B., "A GBAS Landing System Model for Cat I," *Proceedings of the IAIN World Congress*, Inst. of Navigation, Fairfax, VA, 2000.

[18]Etkin, B., and Reid, L. D., *Dynamics of Flight*, 3rd ed., Wiley, New York, 1996.

[19]Houck, S., and Powell, J. D., "Visual, Cruise Formation Flying Dynamics," AIAA Paper 2000-4316, Aug. 2000, URL: http://waas.stanford.edu/~wwu/papers/gps/pubs_chron.html [cited 6 Jan 2003].

[20]Abbott, T., and Elliott, D., "Simulation Evaluation of the Airborne Informtion for Lateral Spacing Concept," NASA TP-2001-210665, Langley, VA, 2001.

[21]"Minimum Aviation System Performance Standards for Automatic Dependent Surveillance Broadcast (ADS-B)," RTCA/Do-242, Washington, DC, Feb. 1998.

[22]Pachter, M., D'Azzo, J. J., and Proud, A. W., "Tight Formation Flight Control," *Journal of Guidance, Control, and Dynamics*, Vol. 24, No. 2, 2001, pp. 246–254; also AIAA Paper 99-4207, Aug. 1999.

[23]Leon-Garcia, A., *Probability and Random Processes for Electrical Engineering*, 2nd ed. Addison Wesley Longman, Reading, MA, 1994.

[24]Lankford, McCartor, Yates, Ladecky, and Templeton, "Comparative Study of Airborne Information Lateral Spacing (AILS) System with Precision Runway Monitor System," DOT-FAAAFS-420-83, Oklahoma City, OK, April 2000.